J. Electromagnetic Analysis & Applications, 2010, 2: 174-182
doi:10.4236/jemaa.2010.23025 Published Online March 2010 (http://www.SciRP.org/journal/jemaa)

Exact Solutions of Equations for the Strongly-Conductive and Weakly-Conductive Magnetic Fluid Flow in a Horizontal Rectangular Channel

Mingjun Li[1], Xinrong Zhang[2], Hiroshi Yamaguchi[3]

[1]School of mathematics and computational Science, Xiangtan University, Xiangtan, China; [2]Department of Energy and Resources Engineering, College of Engineering, Peking University, Beijing, China; [3]Faculty of Mechanical Engineering, Doshisha University, Kyoto, Japan.
Email: limingjun@xtu.edu.cn, alimingjun@163.com

Received April 1st, 2009; revised May 5th, 2009; accepted June 23rd, 2009.

ABSTRACT

This paper presents the results of exact solutions and numerical simulations of strongly-conductive and weakly-conductive magnetic fluid flows. The equations of magnetohydrodynamic (MHD) flows with different conductivity coefficients, which are independent of viscosity of fluids, are investigated in a horizontal rectangular channel under a magnetic field. The exact solutions are derived and the contours of exact solutions of the flow for magnetic induction modes are compared with numerical solutions. Also, two classes of variational functions on the flow and magnetic induction are discussed for different conductivity coefficients through the derived numerical solutions. The known results of the phenomenology of magnetohydrodynamics in a square channel with two perfectly conducting Hartmann-walls are just special cases of our results of magnetic fluid.

***Keywords*:** *Magnetic Fluid, Variational Function, Conductivity Coefficient, Strongly-Conductive, Weakly-Conductive*

1. Introduction

The first classical study of electro-magnetic channel flow was carried out by Hartmann in the 1930s [1]. Hartmann's well-known exact solution can be applied to very closely related problems in magneto-hydrodynamics (MHD) to appreciably simplify physical problems and give insights into new physical phenomena.

In magnetic fluids, the fluid dynamic phenolmena with magnetic induction create new difficulties for the solution of the problems under consideration. The classical Hartmann flow can be further generalized to include arbitrary electric energy extraction from or addition to the flow. In general, classical MHD flows are dealt with using the exact solution of the Couette flow which is presented when the magnetic Prandtl number is unity [1].

The exact solutions of appropriately simplified physical problems provide estimates for the approximate solutions of complex problems. In view of its physical importance, the flow in a channel with a considerable length, rectangular, two-dimensional, and unidirectional cross section, which is assumed steady, pressure-driven of an incompressible Newtonian liquid, is the simplest case to be considered. In such a flow, taking into account the symmetrical planes $y=0$ and $z=0$ and an exact solution is obtained by using the separation of variables. The solution indicates that, when the width-to-height ratio increases, the velocity contours become flatter away from the two vertical walls and that the flow away from the two walls is approximately one-dimensional (the dependence of u_x on y is weak) [2].

If all walls are electrically insulating, $\sigma_w = 0$, Shercliff (1953) has investigated principle sketch of the phenomenology of Magnetohydrodynamics (MHD) channel flow of rectangular cross-section with Hartmann walls and side walls [3]. For perfectly conducting Hartmann walls, $\sigma = \infty$, Hunt (1965) gave velocity profile and current paths for different Hartmann number. They found that the current density is nearly constant in most of channel cross sections, the velocity distribution is flat, and the thickness of the side layers decreases with increasing intensity of $\mathbf{B}$, i.e. increasing Hartmann number [3]. Recently, Carletto, Bossis and Ceber defined the ratio magnetic energy of two

aligned dipoles to the thermal energy $\vartheta = \pi\mu_0\beta^2 a^2 H_0^2 / kT$, and their theory well predicts the experimental results in a constant unidirectional field [4]. Further results can be found in reference [5].

Other flow configurations in basic MHD may include Hele-Shaw cells. Wen *et al*. [6,7] were motivated to visualize the macroscopic magnetic flow fields in a square Hele-Shaw cell with shadow graphs for the first time, taking advantage of its small thickness and corresponding short optical depth. Examples of applications of MHD include the chemical distillatory processes, design of heat exchangers, channel type solar energy collectors and thermo-protection systems. Hence, the effects of combined magnetic forces due to the variations of magnetic fields on the laminar flow in horizontal rectangular channels are important in practice [8–10].

In the present study, we consider the characteristics of magnetic fluids in a horizontal rectangular channel under the magnetic fields and use the flow equations with a conductivity coefficient. The exact solutions of the strongly-conductive and weakly-conductive magnetic fluids are considered using the series expansion technique in order to obtain the relationship between the flow and magnetic induction. Also, a quadratic function on flow and magnetic induction is studied to verify the characteristic of flow field using the obtained solutions.

2. The Exact Solution of the Magnetic Fluid Equations

The configuration of the flow geometry is illustrated in **Figure 1**. The problem considered in this study is an incompressible steady flow in the positive *x*-direction with a magnetic field applied in the positive *z*-direction. The cross-section of the channel is given by the flow region $2a$ and $2b$ while the channel length is $2c$. The system of basic magnetic fluid equations is given as follows [5]

$$\nabla \cdot \mathrm{U} = 0 \tag{1}$$

$$\rho \frac{\mathrm{D}\mathbf{U}}{\mathrm{Dt}} = -\nabla \mathrm{p} + \eta \nabla^2 \mathbf{U} + \mathbf{j} \times \mathbf{B} + (\mathbf{M} \cdot \nabla)\mathbf{H} + \mathbf{M} \times (\nabla \times \mathbf{H}) + \mathbf{F} \tag{2}$$

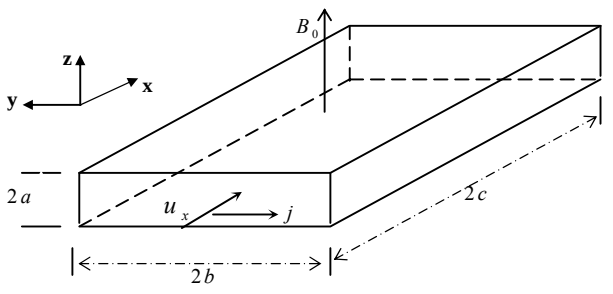

Figure 1. Illustration of flows in a rectangular channel

The Maxwell's equations in their usual form

$$\nabla \cdot \mathbf{B} = 0,\ \nabla \times \mathbf{E} = -\frac{\partial \mathbf{B}}{\partial t},\ \nabla \cdot \mathbf{E} = -\frac{\rho_e}{K_0} \tag{3}$$

with the relation equations and the Ohm's law given as

$$\mathbf{B} = \mu_0 \mathbf{H} + \mathbf{M} = (\mu_0 + \chi_m)\mathbf{H} \tag{4}$$

$$\mathbf{j} = \sigma(\mathbf{E} + \mathbf{U} \times \mathbf{B}) \tag{5}$$

where μ_0 is the permeability of free space, χ_m is the magnetic susceptibility (H/m), σ is the conductivity, $\mathbf{B}$ is the magnetic induction, $\mathbf{H}$ is the magnetic field (A/m), and $\mathbf{M}$ is the magnetization (A/m).

We choose the x axis such that the velocity vector of the fluid is $U = (u_x, 0, 0)$ and from the continuity Equation (1), we have $u_x = u_x(y, z)$. We also choose $\mathbf{B} = \mathbf{B}_0 + \mathbf{b} = (b_x, 0, B_0)$, where B_0 is a constant representing magnetic induction.

Applying the Maxwell's equation $\nabla \cdot \mathbf{B} = 0$ and $\partial b_x / \partial x = 0$, we have $b_x = b_x(y, z)$. To simplify our presentations, the following assumptions are made for related variables:

$$\mathbf{U} = (u_x, 0, 0),\ \mathbf{j} = (0, j_y, j_z) \tag{6}$$

$$\mathbf{E} = (0, E_y, E_z),\ \mathbf{B} = \mathbf{B}_0 + \mathbf{b} = (b_x, 0, B_0) \tag{7}$$

$$\mathbf{H} = (H_x, 0, H_0) \tag{8}$$

$$\mathbf{M} = (M_x, 0, M_0),\ \mathbf{F} = (F_x, 0, 0) \tag{9}$$

And $\nabla \cdot \mathbf{E} = 0$, Equation (3) is satisfied. As there is no excess charge in the fluid, then, by using (5), $\mathbf{j}$ is obtained as follows

$$\mathbf{j} = (0, j_y, j_z) = (0, \sigma(E_y - u_x B_0), \sigma E_z) = (0, \frac{1}{\mu_0}\frac{\partial b_x}{\partial z}, -\frac{1}{\mu_0}\frac{\partial b_x}{\partial y}) \tag{10}$$

$$\frac{\partial \mathrm{E_z}}{\partial \mathrm{y}} = \frac{\partial \mathrm{E_y}}{\partial \mathrm{z}} \tag{11}$$

The magnetic fluid boundary conditions considered here are

$$b_x = 0 \text{ at } y = \pm b,\ z = \pm a$$

$$u_x = 0 \text{ at } y = \pm b,\ z = \pm a$$

We shall also assume that all quantities are independent of time t, that is to say, the fluid we consider here is in a steady state.

2.1 The Strongly-Conductive Fluid

The magnetic fluid is called strongly-conductive if the term $\mathbf{M} \times (\nabla \times \mathbf{H})$ appears [8]. Under the condition of strongly conductive, the coefficient $\mathbf{M} \times (\nabla \times \mathbf{H})$ is much

larger than the Kelvin force density $(\mathbf{M}\cdot\nabla)\mathbf{H}$ so that $\mathbf{J}\times\mathbf{B}$ is considered while $(\mathbf{M}\cdot\nabla)\mathbf{H}$ is neglected. Using the steady-state assumption, *i.e.*, $\partial/\partial t = 0$, Equation (2) can be written as follows

$$\eta\left(\frac{\partial^2 u_x}{\partial y^2}+\frac{\partial^2 u_x}{\partial z^2}\right)=\frac{\partial(p'-f_x')}{\partial x}-(1-\mu_0\chi_m(\mu_0+\chi_m)^{-2})j_y B_0 \tag{12}$$

$$\frac{\partial p'}{\partial y}=j_z b_x \tag{13}$$

$$\frac{\partial p'}{\partial z}=-j_y b_x \tag{14}$$

where $p'=p-1/2\chi_m H_x^2$. Note that Sutton and Sherman [1] gave an incorrect result in their equation (10.85) which should be the above Equation (14).

For Hartmann flow, it is feasible to replace E_y by $\mathrm{K}\bar{u}_x B_0$ for a simple model, then $j_y=\sigma B_0(\mathrm{K}\bar{u}_x-u_x)$ where $\bar{u}_x=\frac{1}{4ab}\int_{-a}^{a}\int_{-b}^{b}u_x(y,z)dydz$.

The axial pressure gradient $-\partial(p'-f_x')/\partial x$ is taken to be $\mathrm{K}\eta'$ if the gravitational field is neglected, and $\partial f_x'/\partial x=0$, where $\eta'=\eta(1-\mu_0\chi_m(\mu_0+\chi_m)^{-2})^{-1}$ is the viscosity of magnetic fluid. Combining Equations (12)–(14) yields

$$\eta'\left(\frac{\partial^2 u_x}{\partial y^2}+\frac{\partial^2 u_x}{\partial z^2}\right)+\frac{B_0}{\mu_0}\frac{\partial b_x}{\partial z}+\mathrm{K}\eta'=0 \tag{15}$$

$$B_0\mu_0\sigma\frac{\partial u_x}{\partial z}+\left(\frac{\partial^2 b_x}{\partial y^2}+\frac{\partial^2 b_x}{\partial z^2}\right)=0 \tag{16}$$

Let

$$u_1=u_x+\frac{b_x}{\mu_0\sqrt{\sigma\eta'}},\quad u_2=u_x-\frac{b_x}{\mu_0\sqrt{\sigma\eta'}} \tag{17}$$

then Equations (15) and (16) are reduced to

$$\frac{\partial^2 u_1}{\partial y^2}+\frac{\partial^2 u_1}{\partial z^2}+\frac{H_a\sqrt{\eta'^{-1}\eta}}{a}\frac{\partial u_1}{\partial z}+\mathrm{K}=0 \tag{18}$$

$$\frac{\partial^2 u_2}{\partial y^2}+\frac{\partial^2 u_2}{\partial z^2}-\frac{H_a\sqrt{\eta'^{-1}\eta}}{a}\frac{\partial u_2}{\partial z}+\mathrm{K}=0 \tag{19}$$

where the Hartmann number H_a is defined as $H_a=B_0 a\sqrt{\sigma\eta^{-1}}$.

The solution for u_1 is obtained by expressing K over the range $-b<y<b$ as a cosine Fourier series,

$$\mathrm{K}=\frac{4k_0}{\pi}\sum_{n=0}^{\infty}\frac{(-1)^n}{2n+1}\cos\frac{(2n+1)\pi y}{2b} \tag{20}$$

where k_0 is a constant. The solution for u_1 is then written

$$u_1=\frac{16Kb^2}{\pi^3}\sum_{n=0}^{\infty}\frac{(-1)^n}{(2n+1)^3}\left[1+\frac{e^{m_1 z}\sin hm_2 a-e^{m_2 z}\sin hm_1 a}{\sin h(m_1-m_2)a}\right] \tag{21}$$

where m_1 and m_2 are given as

$$m_{1,2}=\frac{-H_a\sqrt{\eta'^{-1}\eta}b\pm\sqrt{b^2H_a^2\eta'^{-1}\eta+a^2(2n+1)^2\pi^2}}{2ab} \tag{22}$$

It should be pointed out that the solution for u_2 is just the same function as u_1 in which m_1 and m_2 are displaced by m_3 and m_4, respectively, which are given by

$$m_{3,4}=\frac{H_a\sqrt{\eta'^{-1}\eta}b\pm\sqrt{b^2H_a^2\eta'^{-1}\eta+a^2(2n+1)^2\pi^2}}{2ab} \tag{23}$$

2.2 The Weakly-Conductive Fluid

If the fluid is weakly-conductive and the field $\mathbf{E}$ is not time-dependent, the term $\mathbf{M}\times(\nabla\times\mathbf{H})$ will disappear as shown in equations (104) [8]. Considering Equation (2) through (4) and making use of the assumptions mentioned above, the following relations are obtained,

$$\eta\left(\frac{\partial^2 u_x}{\partial y^2}+\frac{\partial^2 u_x}{\partial z^2}\right)=\frac{\partial(p-f_x')}{\partial x}-j_y B_0 \tag{24}$$

$$\frac{\partial p}{\partial y}=j_z b_x \tag{25}$$

$$\frac{\partial p}{\partial z}=-j_y b_x \tag{26}$$

Replacing E_y with $\mathrm{K}\bar{u}_x B_0$, we have $j_y=\sigma B_0(\mathrm{K}\bar{u}_x-u_x)$ as well as in Subsection 2.1. Then, as the axial pressure gradient $-\partial(p-f_x')/\partial x$ is taken to be $K\eta$, where

$$K=\frac{4k_0}{\pi}\sum_{n=0}^{\infty}\frac{(-1)^n}{2n+1}\cos\frac{(2n+1)\pi y}{2b} \tag{27}$$

where k_0 is a constant. Let

$$u_1=u_x+\frac{b_x}{\mu_0\sqrt{\sigma\eta}},\quad u_2=u_x-\frac{b_x}{\mu_0\sqrt{\sigma\eta}} \tag{28}$$

Thus, the solution of Equation (28) for u_1 as in (17) is also obtained

$$u_1=\frac{16Kb^2}{\pi^3}\sum_{n=0}^{\infty}\frac{(-1)^n}{(2n+1)^3}[1+$$

$$\frac{e^{m_1 z}\sin hm_2 a - e^{m_2 z}\sin hm_1 a}{\sin h(m_1 - m_2)a}]\times\cos\frac{(2n+1)\pi y}{2b} \quad (29)$$

where m_1 and m_2 are as follows

$$m_{1,2} = \frac{-H_a b \pm \sqrt{H_a{}^2 b^2 + a^2(2n+1)^2\pi^2}}{2ab} \quad (30)$$

Note that the solution for u_2 is the same function as u_1 in which m_1 and m_2 are given as follows

$$m_{3,4} = \frac{H_a b \pm \sqrt{H_a{}^2 b^2 + a^2(2n+1)^2\pi^2}}{2ab} \quad (31)$$

For a weak-conductive fluid, its solution is simply the solution of the conductive fluid with a conductive coefficient $\lambda = \sqrt{\eta'^{-1}\eta} = 1.0$ (for $\mu_0 = 0$). We find that $\lambda = \sqrt{\eta'^{-1}\eta} = \sqrt{1-\mu_0\chi_m(\mu_0+\chi_m)^{-2}}$ which is obviously independent of the fluid viscosity.

2.3 Unidirectional Two Dimensional Flow without a Magnetic Field

Here we only consider a unidirectional two dimensional flow without a magnetic field, so that $H_a = 0$, Equations (18) and (19) are reduced to

$$\frac{\partial^2 u_x}{\partial y^2} + \frac{\partial^2 u_x}{\partial z^2} + K = 0 \quad (32)$$

The boundary conditions are as follows

$$\frac{\partial u_x}{\partial y} = 0 \quad \text{at} \quad y = -b \quad (33)$$

$$\frac{\partial u_x}{\partial z} = 0 \quad \text{at} \quad z = -a \quad (34)$$

$$u_x = 0 \quad \text{at} \quad y = b, \quad z = a \quad (35)$$

In order to obtain an exact solution of Equation (32), comparing with our above results, we have

$$K = \frac{4k_0}{\pi}\sum_{n=0}^{\infty}\frac{(-1)^n}{2n+1}\cos\frac{(2n+1)(y+b)\pi}{2b} \quad (36)$$

where k_0 is a constant. The problem consisting Equation (32) and its conditions are solved similarly using the separation of variables, which has the solution as follows [9]

$$u_x(y,z) = \frac{Ka^2}{2}(1-(\frac{z+a}{2a})^2 + 4\sum_{n=0}^{\infty}\frac{(-1)^n}{a_n^3}\cosh[\frac{a_n(y+b)}{2a}]$$

$$[\cosh(\frac{a_n b}{2a})]^{-1}\cos[\frac{a_n(z+a)}{2a}] \quad (37)$$

where

$$a_n = (2n-1)\frac{\pi}{2}, \quad n = 1,2,\cdots \quad (38)$$

2.4 The Solutions, Flow Field and Discussions

In the present study, the flow fields and their associated functions are presented in the flow region with $a = 1$, $b = 1$. Since H_a ranges from 10 to 100 in most practical problems, the initial magnetic induction is taken to be $B_0 = 10$ (kg.s^{-2}.A^{-1}), $\mu_0 = 4\pi 10^{-7}$ (H/m), $H_a = 50$ and the constant $k_0 = 10$.

Figure 2 depicts the solutions for $\lambda = 0.02$, 0.2 and 1.0, where $\lambda = \sqrt{\eta'^{-1}\eta}$ is the conductivity coefficient. The velocity contours are displayed in **Figure 2(a)** for different values of the conductivity coefficient. It is shown that the velocity gradients become larger gradually near four vertical walls as the conductivity coefficient increases for different magnetic fluids. On the contrary, in the region of (0,0), the velocity gradients lower gradually as the conductivity coefficient increases. For the case of a constant Hartmann number, the magnetic fluid are shown in **Figure 2(b)** for different values of the conductivity coefficient, and as indicated, the strength of magnetic induction dampens horizontal away from the plane $z = 0$ and the walls $z = \pm 1$ as the conductivity coefficient increases. On the contrary, near the walls $y = \pm 1$, the magnetic induction becomes gradually low as the conductivity coefficient increases. For conductivity coefficient $\lambda = 0.02$, the flow contours are similar to those in the reference[10] for the magnetic Rayleigh number $Ram = 0.0$ and the Rayleigh number $Ra = 1{,}000$. Our analysis shows that the flow field changes with different conductivity coefficients.

Figure 3 shows the velocity fields for steady, unidirectional flows in a rectangular channel and K is a cosine Fourier series of y and conductivity coefficient $\lambda = 0$. The velocity contours are similar to those given by Papanastasiou et *al*. for the width-to-height ratio 1:1 [2].

In **Figures 4(a)** and **4(b)**, the development of the velocity profile in y and z directions are shown for various values of the conductivity coefficient λ. For the symmetry, we only consider two cases: (a) $0 \le y \le b$, $-a \le z \le a$; and (b) $0 \le z \le a$, $-b \le y \le b$. Several interesting observations are readily made from the results. The cooperate process of y and z is shown in the above analysis. In order to clearly show the self-governed process of y and z, the contours of the velocity versus coordinate y, and the velocity versus coordinate z are given. It is clear that the velocity gradients increase quickly near the boundary walls $z = \pm a$ and $y = \pm b$ as λ is increased. On the other hand, the exact solutions are multiple hyper-cosine functions of z, and cosine functions of y. Therefore, the velocity gra-

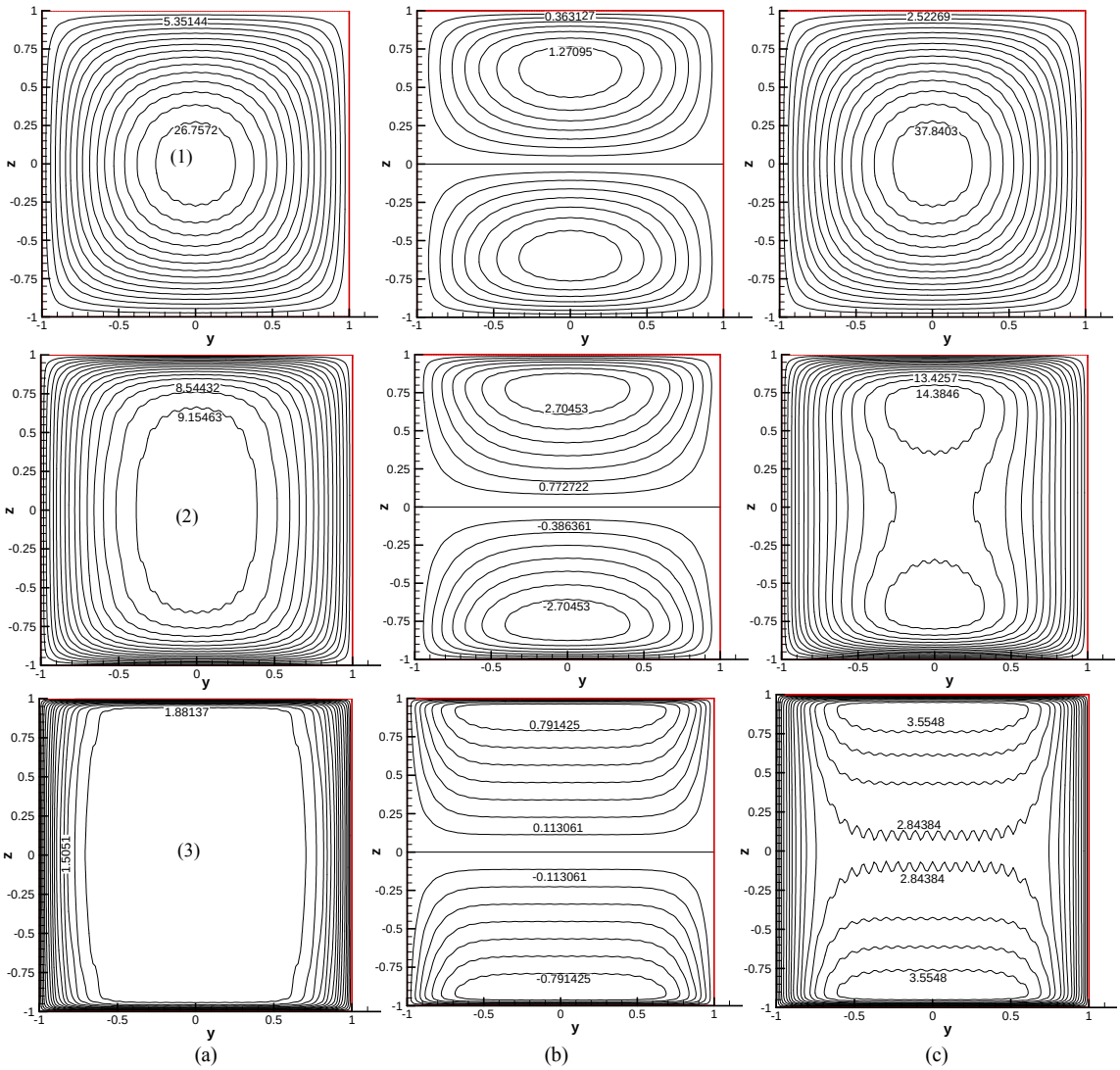

Figure 2. The distribution of flow field and magnetic induction. (a) Velocity contours u_x; (b) Magnetic induction distributions b_x; and (c) The velocity composition function F. (1) $H_a = 50$, $\lambda = 0.02$; (2) $H_a = 50$, $\lambda = 0.2$; and (3) $H_a = 50$, $\lambda = 1.0$

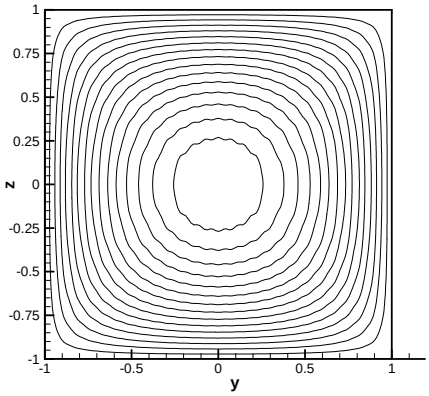

Figure 3. Velocity field with a cosine Fourier series K of y for conductive coefficient $\lambda = 0$

dient is larger near the boundary walls $y = \pm b$ than that near the boundary walls $z = \pm a$ for a given λ.

For a given Hartmann number, comparing **Figure 2** of this paper with Figures 3.2, 3.3 and 3.4 of Reference [3], current density distribution magnetic fluid and magneto-hydrodynamics (MHD) are the same. Comparing **Figure 2** of this paper with Figure 3.1 of Reference [3], the velocity profile of the phenomenology is also same for magnetic fluid and MHD. Of course, magnetic fluid and MHD have different equations and formulations of the Hartmann number. For magnetic fluid, the constitutive equation is $\mathbf{B} = \mu\mathbf{H} + \mathbf{M}$, the Hartmann number $H_a = \mathrm{B}_0 a\sqrt{\sigma\eta^{-1}}$ and conductivity coefficient λ are introduced in our work. The flow and magnetic induction

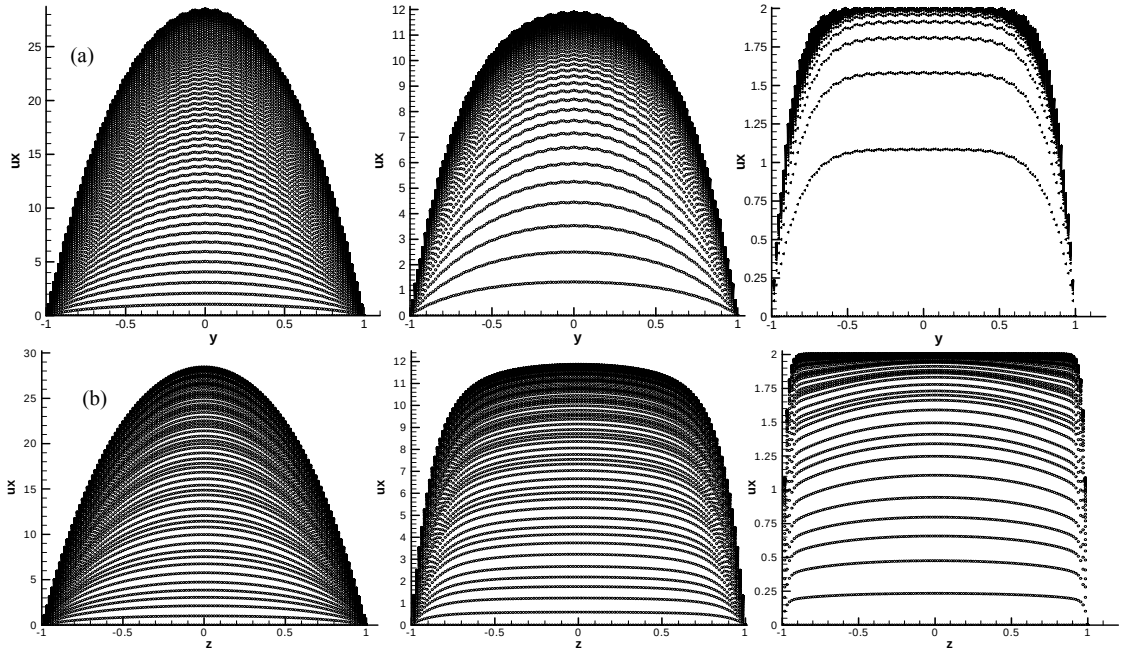

Figure 4. The development of the velocity profile (a) The u_x vs y-axis; (b) u_x vs z-axis. (1) $H_a = 50$, $\lambda = 0.02$; (2) $H_a = 50$, $\lambda = 0.2$; (3) $H_a = 50$, $\lambda = 1.0$

change with different λ. Differently, in MHD, Shercliff and Hunt considered the induction equation $\frac{\partial \mathbf{B}}{\partial t} + (\mathbf{V}\cdot\nabla)\mathbf{B} = \frac{1}{\mu\sigma}\nabla^2\mathbf{B} + (\mathbf{B}\cdot\nabla)\mathbf{V}$ and used only the linear constitutive equation $\mathbf{B} = \mu\mathbf{H}$ with Hartmann number $H_a = LB_0\sqrt{\sigma/\rho\mu}$. They gave velocity profile and current paths for different Hartmann number.

3. Two Class of Variational Functions on the Flow and Magnetic Induction

For many years the variation techniques have been effectively applied to problems in the theory of elasticity. However, they are rarely used in fluid dynamic problems. The great utility in elasticity problems are due to the fact that they can be conveniently applied to linear problems. This, of course, explains why they are not frequently used in fluid dynamics since most such problems are nonlinear [10,11].

For the conductive fluid problems of the type being considered here, we recall the governing Equations (15) and (16) which are linear for u_x and b_x and the variation technique may be tried. Firstly, consider the following integral [12]

$$I(u_x, b_x; \lambda) = \iint_s F(y, z, \lambda; u_x, b_x, \lambda)dydz \qquad (39)$$

where F is some given function of u_x, b_x, λ. Clearly, the value of the integral depends on the choice of the functions $u_x(y,z,\lambda)$, $b_x(y,z,\lambda)$ and λ. Now, let us pose the following problem: to obtain functions u_x, b_x and λ to minimize the value of I. As is well known from variational calculus, the necessary conditions that u_x, b_x and λ for minimized I are the Euler equations:

$$\frac{\partial F}{\partial y} - \frac{\partial}{\partial y}(\frac{\partial F}{\partial u_x}) - \frac{\partial}{\partial y}(\frac{\partial F}{\partial b_x}) = 0 \qquad (40)$$

$$\frac{\partial F}{\partial z} - \frac{\partial}{\partial z}(\frac{\partial F}{\partial u_x}) - \frac{\partial}{\partial z}(\frac{\partial F}{\partial b_x}) = 0 \qquad (41)$$

$$\frac{\partial F}{\partial \lambda} - \frac{\partial}{\partial \lambda}(\frac{\partial F}{\partial u_x}) - \frac{\partial}{\partial \lambda}(\frac{\partial F}{\partial b_x}) = 0 \qquad (42)$$

3.1 Decomposition and Composition Functions on the Flow and Magnetic Induction

Simply, let the parameters be fixed at λ, then $s = [-a, a] \times [-b, b]$. According to u_1 and u_2 in the Equation (17), we only considered the function of u_x, b_x and λ in order to minimize the special function as follows

$$F = ((u_a)^2 + (u_b)^2)^{1/2}$$

$$= \frac{1}{2}((u_x + \frac{b_x}{\mu_0\sqrt{\sigma\eta}})^2 + (u_x - \frac{b_x}{\mu_0\sqrt{\sigma\eta}})^2)^{1/2} \quad (43)$$

where $u_x = u_x(y,z,\lambda)$ and $b_x = b_x(y,z,\lambda)$ are considered as the function of y, z and $\lambda = \sqrt{\eta'^{-1}\eta}$, $-a \le z \le a$, $-b \le y \le b$, and $0 < \lambda_1 < \lambda < \lambda_2$.

Let $u_a = u_1/2 = (u_x + \tilde{c}b_x)/2$, $u_b = u_2/2 = (u_x - \tilde{c}b_x)/2$, then $u_x = u_a + u_b$. The expressions of u_a and u_b are called the velocity decompositions of the magnetic induction b_x and the flow field u_x with a variable coefficient $\tilde{c}$ of the flow and the magnetic induction, where $\tilde{c} = (\mu_0\sqrt{\sigma\eta})^{-1}$. From **Figure 5**, it is easy to show that $u_a \to u_x/2$, $u_b \to u_x/2$, and $F \to \sqrt{2}/2u_x$ as $b_x \to 0$, where F is the velocity composition of the flow field and the magnetic induction.

It is also easy to know that $F = F(y,z,\lambda)$ has the same variation characteristic as the following function

$$\tilde{F} = (u_x + \frac{b_x}{\mu_0\sqrt{\sigma\eta}})^2 + (u_x - \frac{b_x}{\mu_0\sqrt{\sigma\eta}})^2 \quad (44)$$

The differential of $\tilde{F}$ on λ is given by

$$\tilde{F}_\lambda = 2(u_x u'_{x,\lambda} + \frac{b_x}{\mu_0\sqrt{\sigma\eta}} b_x b'_{x,\lambda}) \quad (45)$$

It is obvious that $\tilde{F}_\lambda$ is a nonlinear function of λ, and is very complex to study the variation characteristics of $\tilde{F}$ by using the method of mathematical analysis.

With Equation (45), the variation characteristics of the function $\tilde{F}$ is determined by flow and magnetic induction as a function of λ.

3.2 A Total Energy Variational Function on the Flow and Magnetic Induction

Based on the above analysis of Equation (17), let $u_1 = u_x + \tilde{c}b_x$, $u_2 = u_x - \tilde{c}b_x$ with $\tilde{c} = (\mu_0\sqrt{\sigma\eta})^{-1}$, we call $\tilde{c}b_x$ the velocity of magnetic fluid flow, which is equivalence to the velocity of magnetic fluid flow evoked by magnetic force. A total energy function is defined by

$$e = e_1 + e_2 = \frac{1}{2}\rho u_x^2 + \frac{1}{2}\rho(\tilde{c}b_x)^2 \quad (46)$$

where e_1 is the kinetic energy, e_2 is the magnetic energy.

By the calculus of variations, we have

$$e'_\lambda = e'_{1,\lambda} + e'_{2,\lambda} = \rho u_x u'_{x,\lambda} + \rho\tilde{c}b_x b'_{x,\lambda} \quad (47)$$

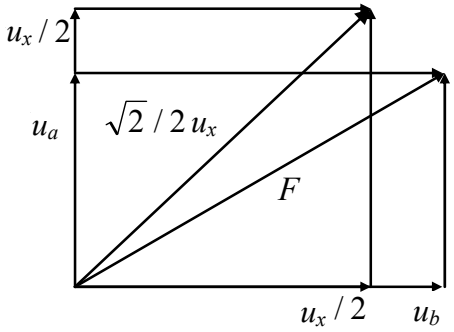

Figure 5. The sketch map of the composition function F of flow and magnetic induction

As u_x and b_x are nonlinear functions of λ, it is very complex to study the variational characteristics of e'_λ by using the method of mathematical analysis.

3.3 Numerical Calculations and Discussions

As seen in **Figures 2(a)** and **2(c)**, in a region of (0,0), the contour of the function F is more similar to that of the flow for $\lambda = 0.02$. Furthermore, the gradient of flow which is larger than that of magnetic induction, the distribution value of F is largely affected depending on the flow. On the contrary, for $\lambda = 1.0$, the gradient of magnetic induction is larger than that of flow as F is largely affected depending upon the gradient of the magnetic induction.

It is observed that the difference of flow and magnetic induction are almost the same for $\lambda = 0.2$ in a region of (0,0), where the distribution of the function F is determined by the gradients of both the magnetic induction and the flow in this region. Furthermore, near $y = \pm 1$ and $z = \pm 1$ for any λ, the difference of flow is acute singularly and the function F is also changed singularly. It is noted that F has only one limit point for $\lambda < 0.2$, and F has two limit points for $\lambda > 0.2$.

As seen in **Figure 6**, the gradient of the total energy is decided by the kinetic energy in the region (0,0) for different values of λ, and near $y = \pm 1$ and $z = \pm 1$ for $\lambda = 0.02$. That is to say, the gradient of the magnetic energy is very large near $z = \pm 1$ for $\lambda = 0.02$, and its value is very small which does not affect the gradient of the total energy. Then, the gradient of the total energy will be affected by the magnetic energy near $z = \pm 1$ for $\lambda = 0.2$ and it will be affected by the magnetic energy near $y = \pm 1$ and $z = \pm 1$ for $\lambda = 1.0$.

4. Concluding Remarks

1) For magnetic fluid of this work and Magnetohydrodynamics (MHD) of Reference [3], the constitutive equa-

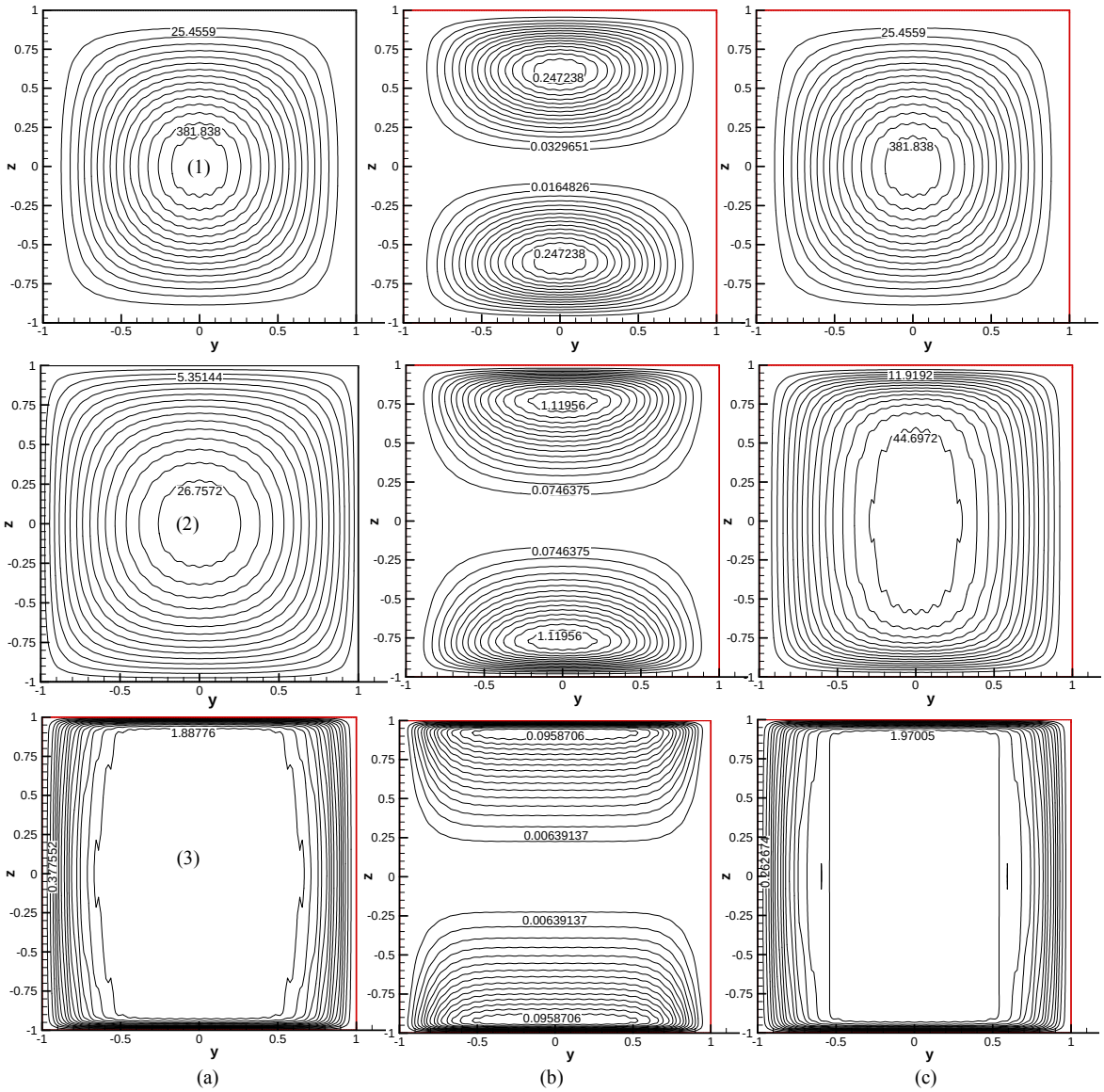

Figure 6. Illustration of energy function (a) The kinetic energy e_1; (b) The magnetic energy e_2; and (c) The total energy e. (1) $H_a = 50$, $\lambda = 0.02$; (2) $H_a = 50$, $\lambda = 0.2$; (3) $H_a = 50$, $\lambda = 1.0$

tions are different, the Hartmann numbers are also different. For magnetic fluid, conductivity coefficient λ is an important coefficient to analyze the flow and the current. For MHD, Hartmann number H_a is the controlling coefficient, Shercliff and Hunt studied velocity profile and current paths for different Hartmann number [3–5].

2) For conductivity coefficient $\lambda = 0$, the velocity contours for steady unidirectional flow is shown in a rectangular channel with K a cosine Fourier series function of y. Our result is in agreement with published findings.

3) A velocity decomposition and composition function F, and a total energy variational function e, on the flow and magnetic induction are considered. The variational characteristics of F are analyzed only using the characteristics of the resultant flow field and the magnetic induction, and the number of its limit points changes as λ changes. It is shown in numerical simulations that the gradient of total energy e is affected by the kinetic energy and the magnetic energy as λ changes.

4) Theoretically, the strongly-conductive and weakly-conductive magnetic fluid flows are studied on different conductivity coefficients which are independent of fluid viscosity in a horizontal rectangular channel.

Table 1. Nomenclature

a	channel length	H_a	Hatmann number
b	channel height	K	dimensionless variable $E_y / \overline{u}_x B_0$
c	channel width	k_0	constant
B	magnetic induction	**M**	magnetization (A/m)
B_0	initial magnetic filed	M_0	initial magnetization
b_x	magnetic induction of x -direction	M_x	magnetization of x -direction
$\widetilde{c}$	coefficient $\widetilde{c} = (\mu_0 \sqrt{\sigma\eta})^{-1}$	u_x	velocity of x -direction
E	electric field with respect to Lab.	$\overline{u}_x$	average velocity
e	total energy	u_1	first exact solution
e_1	kinetic energy	u_2	second exact solution
e_2	magnetic energy	χ_m	the magnetic susceptibility
F	velocity composition function	μ_0	the magnetic susceptibility
F	force on a particle	σ	conductivity
H	magnetic field(A/m)	η	viscosity of fluid
H_0	initial magnetic field	η'	the correctional viscosity of fluid
H_x	magnetic field of x -direction	λ	conductive coefficient $\lambda = \sqrt{\eta'^{r-1}\eta}$

5. Acknowledgments

This work was supported in part by a grant to the research Centre for Advanced Science and Technology at Doshisha University from the Ministry of Education, Japan; the National Natural Science of China (10771178, 50675185, 10676031); the Research Fund for the Doctoral Program of Higher Education (20070530003), Program for New Century Excellent Talents in University (NCET 06-0708)and the Scientific Research Foundation for the Returned Overseas Chinese Scholars of State Education Ministry of China. The authors thank readers for giving references [3–5] and suggestions on comparison with analytical solutions.

REFERENCES

[1] G. W. Sutton and A. Sherman, "Engineering Magnetohydrodynamics," McGraw-Hill Book Company, New York, 1965.

[2] T. C. Papanastasiou, G. C. Georgiou, and A. N. Alexandrou, "Viscous fluid flow," CRC Press LLC, New York, 2000.

[3] U. Mueller and L. Buehler, "Magnetofluiddynamics in channel and containers," Springer-Verlag, Berlin, 2001.

[4] P. Carletto, G. Bossis, and A. Cebers, "Structures in a magnetic suspension subjected to unidirectional and rotating field," International Journal of Modern Physics B, Vol. 16, No. 17–18, pp. 2279–2285, 2002.

[5] E. Blums, A. Cebers, and M. M. Maiorov, "Magnetic fluids," Walter de G Gruyter, Berlin, 1997.

[6] C.-Y. Wen and W.-P. Su, "Natural convection of magnetic fluid in a rectangular Hele-Shaw," Journal of Magnetism and Magnetic Materials, Vol. 289, pp. 299–302, March 2005.

[7] C.-Y. Wen, C.-Y. Chen, and S.-F. Yang, "Flow visualization of natural convection of magnetic fluid in a rectangular Hele-Shaw cell," Journal of Magnetism and Magnetic Materials, Vol. 252, pp. 206–208, November 2002.

[8] R. E. Rosensweig, "Ferrofluids: Magnetically controllable fluids and its applications," In: S. Odenbach, Ed., Basic Equations for Magnetic Fluids with Internal Rotations, Springer-Verlag, New York, p. 61, 2002.

[9] T. H. Kuehn and R. J. Goldstein, "An experimental study of natural convection heat transfer in concentric and eccentric horizontal cylindrical annuli," ASME Journal of Heat Transfer, Vol. 100, pp. 635–640, 1978.

[10] H. Yamaguchi, Z. Zhang, S. Shuchi, and K. Shimad, "Heat transfer characteristics of magnetic fluid in a partitioned rectangular box," Journal of Magnetism and Magnetic Materials, Vol. 252, pp. 203–205, November 2002.

[11] G. B. Arfken and H. J. Weber, "Mathematical methods for physicists," 6th Edition, Elsevier Academic Press, New York, p. 1037, 2005.

[12] H. Yamaguchi, "Engineering fluid mechanics," Springer-Verlag, New York, 2008.

